

NBSIR 81-1651

NBS
PUBLICATIONS

REFERENCE

NATL INST. OF STAND & TECH



A11107 104708

THERMAL CONDUCTIVITY OF A CONCRETE MORTAR FROM 95 K TO 320 K

L. L. Sparks

Thermophysical Properties Division
National Engineering Laboratory
National Bureau of Standards
Boulder, Colorado 80303

PREPARED FOR:
Maritime Administration
Department of Commerce
Washington, D.C. 20235

QC
100
.U56
81-1651
1981

October 1981

NBSIR 81-1651

NATIONAL BUREAU
OF STANDARDS
LIBRARY

DEC 7 1981

Not Rec. - Circ.

Q. 100

5-2-81

100-1-100-1

1981

C. 2

THERMAL CONDUCTIVITY OF A CONCRETE MORTAR FROM 95 K TO 320 K

L L Sparks

Thermophysical Properties Division
National Engineering Laboratory
National Bureau of Standards
Boulder, Colorado 80303

PREPARED FOR:
Maritime Administration
Department of Commerce
Washington, D.C. 20235

October 1981



THERMAL CONDUCTIVITY OF A CONCRETE MORTAR FROM 95 K TO 320 K*

L. L. Sparks
Thermophysical Properties Division
National Bureau of Standards
Boulder, CO 80303

The thermal conductivity of a single concrete mortar specimen with varying moisture content is reported in the temperature range from 95 to 320 K. The measurements were made in a guarded-hot-plate apparatus (ASTM C-177). Moisture migration caused by temperature gradients was minimized by studying the saturated specimen in the low-temperature region. Specimen moisture content and concomitant thermal conductivity were altered by imposing low-pressure, high-temperature conditions on the specimen. The effect of changing the moisture content is discussed.

Key words: concrete; guarded hot plate; low temperature; moisture migration; mortar; porous solid; thermal conductivity.

1. INTRODUCTION

The low-temperature thermal conductivity (λ) of concrete is becoming an increasingly important property due to the use of the material to contain and transport cryogenic fuels. A very limited amount of low-temperature data are available for use by designers of facilities such as ground-based storage tanks, sea-going tankers, barges, and pipelines. The variability of existing data is appreciable due to both the large number of variables which affect λ and to the experimental methods used to determine λ . Perhaps the most difficult part of finding a meaningful λ for moist concrete is that, even for a given composition or mix design, the moisture content and distribution change with time. The thermal gradient necessary in the measurement of λ also establishes a moisture gradient in the specimen: moisture migrates toward the cooler part of the specimen. Since a relatively long time, generally 1 to 4 hours, is required to establish the thermal equilibrium needed for a steady state type of λ determination, both distribution and absolute amount of evaporable moisture may change. This moisture problem is generally circumvented by using either a nonsteady state type of measurement so that the time required to make a measurement is reduced to the point that the effect of migration and evaporation are thought to be small or by making the measurements on a specimen whose evaporable moisture has been removed. Neither of these alternatives is completely satisfactory. The transient methods are not of an absolute nature and result in data with larger uncertainties. Moisture-free concrete is seldom encountered outside the laboratory and excludes a significant factor in λ of real concrete structures, i.e., moisture content.

Both of the above objections can be avoided by cooling and maintaining the specimens at a temperature below the freezing point of the evaporable water and by making the measurements in a guarded-hot-plate system. In the solid phase evaporation and migration don't occur, and time consuming absolute measurements can be made.

The conditioning and testing procedure used on the current specimens was intended to minimize the moisture migration problem and to allow observation of the effect of variable moisture content on λ . The moisture content of the specimens during the experiment was estimated from mass determinations just before installation in the apparatus, immediately after the system was opened, and after oven drying. After installation, the temperature of the saturated specimens was lowered to cryogenic temperatures where the evaporable moisture was in the solid phase. A series of tests were made with the highest test temperatures below 273 K. The specimens were then warmed to ambient temperature for an extended period to allow for migration and some drying. This conditioning was followed by a second set of λ measurements. The third and final specimen condition was achieved by holding the specimens at approximately 340 K and reduced pressure for several days. This procedure was followed by a third set of λ determinations.

*This work was done for the Department of Commerce, Maritime Administration, Department of Commerce Building, Washington, DC 20235, under Program 193000, Project 12-410-54-425.

2. APPARATUS

The apparatus used to make the λ measurements is shown schematically in figures 1 and 2. The path of the cooling fluid is shown in figure 1 and the details of the specimen configuration are shown in figure 2. This type of system is commonly known as a guarded-hot-plate and is described in the American Society for Testing and Materials Standard C177 (ASTM, 1978). This method allows an absolute determination of λ and is considered to be the most accurate method available for many materials. The particular apparatus used to make the λ measurements reported here is described in detail by Smith, Hust, and Van Poolen (1981); a very brief description is included below.

The basic operation of this type of apparatus involves supplying a measured amount of power, Q , from the main heater plate to the two specimens and measuring the resulting steady-state temperature difference. The thermal conductivity is then given by

$$\lambda = \frac{\Delta X}{2A} \times \frac{Q}{\Delta T} \quad (1)$$

where ΔX is the sample thickness, A the area of the metered section of the main heater plate, and ΔT is the steady-state mean temperature difference across the specimens. The absolute temperatures and temperature differences are measured with type K thermocouples.

The accuracy of the λ results are dependent on measurement of the parameters shown in eq (1) and on establishing unidirectional (vertical in this case) heat flow in the metered area of the specimens. The inner-guard heater plate is controlled at the temperature of the main heater in order to minimize radial heat flow in the metered area. Somers and Cyphers (1951) and ASTM C177 indicate that when the diameter to thickness ratio is approximately 4, the errors in λ due to nonvertical heat flow should be less than 1%.

The most critical and difficult parameters to determine are the specimen temperature differences (ΔT) which averaged 10 K for the concrete mortar. The correctness of ΔT measurements depends on plate-to-specimen thermal contact, on unidirectional heat flow, and on thermocouple calibration and referencing sources of error. The diverse materials which can be tested in this type of system cause a wide range of plate-to-specimen contact situations. Tye and Spinney (1976) found that embedding the thermocouple wires in concrete, as opposed to the measuring plates, resulted in higher calculated conductivities. This effect resulted from better specimen-to-thermocouple contact which resulted in smaller measured ΔT and concomitant larger λ (eq (1)). They also found that the effect of thermocouple placement was dependent on the conductivity of the specimens. As the conductivity of the specimen increases, the relative effect of an air gap in the specimen-to-plate interface becomes larger.

Thermocouple placement used in obtaining the data reported below consisted of cementing the wires into machined grooves in the measuring plates so that the top of the wires were flush with the plate surfaces. Small matching grooves were machined in the concrete surfaces to protect the wires from physical abrasion and to minimize the effect of possible high points in the placement of the thermocouples. Corrections were made in the area term of eq (1) to account for the grooves in the concrete.

The accuracy of measurements made with this system on fiberglass and fiberboard reference materials is discussed by Smith, et al. (1981). As mentioned above, the specimen to thermocouple contact is critical and material dependent so that the systematic uncertainties found for fibrous materials cannot be applied directly to the concrete measurements. Because of the rigid, nonconforming nature of the concrete, the specimen-to-plate contact would not be as good for concrete specimens as for fiber-type materials. Less than perfect contact would tend to make ΔT too large and λ too small. Based on the percentage errors given by Smith for each parameter in eq (1) and the magnitude of these parameters for the concrete experiments, uncertainties for concrete are estimated to be 0.004 W/m·K random and 0.010 W/m·K systematic near room temperature; near 80 K the random component is 0.003 W/m·K and the systematic uncertainty is 0.013 W/m·K.

3. MATERIAL

Commercially important portland cements are available in a variety of compositions, but all are composed primarily of reactive calcium silicates or calcium aluminates. When mixed with water these materials form insoluble hydration products, and make up a class known as hydraulic cements. The thermal and mechanical properties of mortars or concretes made using hydraulic portland cement are influenced by cement composition, cement content, type, size, and amount of aggregate, water to cement ratio, age and aging environment.

The material used here is a mortar with (water mass)/(cement mass) equal to 0.5 and (aggregate mass)/(cement mass) equal to 3.38. An air entraining agent, neutralized resin, was included in the mix. Computed air content of the plastic mortar was 17.7 percent and the density was 1.9 g/cm³ (ASTM C138).

The petrographic analysis of the aggregate, locally known as Clear Creek Sand, is shown in table 1. The sieve analysis of the aggregate is given in table 2. This size distribution results in a fineness modulus of 3.26. The chemical analysis of the type I portland cement is shown in table 3. The relative fineness, ASTM C204, as determined by the Blaine air permeability technique, is 4185 cm²/g and the initial and final setting times are 2 and 3.67 hours respectively as determined by the Gilmore needles technique, ASTM C266.

Table 1. Petrographic analysis of Clear Creek Sand (Monk, 1975)

Rock and mineral types	Percentage by particle count		
	No. 8	No. 16	No. 30 ^a
Granites, includes some quartz monzonites	67.4	66.4	33.2
Metamorphics; includes schists and gneisses	7.2	3.7	1.5
Altered volcanics; includes rhyolites, andesites, andesitic basalts and basalts	6.8	2.7	1.8
Quartz (pebbles and vein quartz)	12.4	17.2	44.9
Feldspar (clear, white, and pink)	5.7	7.2	15.9
Micas (muscovite and biotite)	--	0.7	0.8
Sillimanite	0.3	1.7	1.5
Epidote	0.2	0.2	--
Magnetite	--	0.2	0.1
Garnet	--	--	0.1
Chert (includes some cryptocrystalline quartz)	--	--	0.2

^a The coarse sand, retained on a number 30 sieve, is angular to subangular and contains 54 percent elongated and flattened particles. Sand passing through the number 30 sieve is angular in shape, contains 3 percent flattened and elongated particles, and contains decreasing amounts of fine grained rock types such as those found in the coarse sand. Increasing amounts of monomineralic grains of quartz, feldspar, micas, amphiboles, epidote, magnetite, garnet, sillimanite, and miscellaneous detrital minerals are found in the sand passing the number 30 sieve.

Table 2. Sieve analysis of the Clear Creek Sand used in NBS mortar specimens

Sieve		Percent Passing	Cumulative Percent retained
Number	Size (mm)		
4	4.75	99.4	0.6
8	2.36	80.5	19.5
16	1.18	59.4	40.6
30	0.60	28.6	71.4
50	0.30	6.6	93.4
100	0.15	0	100

Table 3. Chemical analysis and computed compound makeup of the portland type I cement used in NBS mortar specimens (Trujillo, 1980)

<u>Chemical Analysis</u>	<u>Weight Percent</u>
SiO ₂	21.16
Al ₂ O ₃	5.24
Fe ₂ O ₃	2.64
CaO	63.69
MgO	1.84
SO ₃	2.88
Na ₂ O	0.27
K ₂ O	0.68
Na ₂ O equivalent	0.72
insoluble residue	0.21
loss on ignition ^a	1.41
<u>Computed Compounds^b</u>	
C ₃ S	51.2
C ₂ S	22.1
C ₃ A	9.4
C ₄ AF	8.0

^a Loss on ignition (ASTM C114) is used to specify moisture and CO₂ content. Weight change includes a correction for increased SO₃ due to ignition.

^b Calculated, assumed compounds using commonly accepted abbreviations (ASTM C150): C = CaO, S = SiO₂, A = Al₂O₃, and F = Fe₂O₃.

The specimens were formed, ASTM C192, in lucite molds. Twenty-four hours after forming, they were removed from the molds and immersed in a saturated lime water bath controlled at 296 K. They remained in this environment, except for brief periods for measurement and machining, until being installed in the λ system. The age of the specimens at the beginning of the test period was 63 days. The thermal conductivity specimens were sawed from a 30.5 cm tall by 20.3 cm diameter cylinder of concrete. The machining consisted of sawing adjacent, nominal 2.54 cm thick wafers from the bulk supply. The flat faces of the wafers were polished and ground flat and parallel using a surface grinder. Machining required 6.5 hours and was done after the specimens had aged 28 days. The specimens were returned to the conditioning bath after machining.

The thicknesses of the saturated specimens were 2.540 cm for the upper specimen and 2.538 cm for the lower specimen (see fig. 2). The average density of the aged specimens in the saturated-surface-dry (SSD) condition was 1.869 g/cm³. After the thermal conductivity experiment, the specimens were oven dried at approximately 378 K until there was no further weight loss: the moisture free average density was 1.686 g/cm³. The average evaporable moisture in the specimens, when in SSD condition, was 10.8 percent of the average, oven-dry specimen weight.

Weight measurements made during the dimensional measuring process indicated that, when exposed to ambient conditions, the specimens lose evaporable moisture at a rate of about 3 percent of the initial evaporable moisture per hour. This loss rate, applied to the time interval required to install the specimens in the thermal conductivity system and reduce their temperature to 269 K, leads to a moisture content of 140.5 g per specimen or 10.4 percent of the oven dry specimen weight. The assumptions involved in arriving at this average moisture content are that (1) rate of loss is the same as observed on the same specimens at an earlier date, (2) the loss rate is proportional to the exposed surface area, and (3) the moisture loss ceased when the maximum specimen temperature was below 269 K. The freezing temperature of the evaporable liquid in the pores of the specimens is lower than this, but a sealing effect due to free surface freezing essentially stops net moisture loss near 269 K. Redistribution of moisture within the capillaries and pores due to gravity and the temperature gradient would continue at a decreasing rate until about 200 K is reached. At approximately this temperature most evaporable moisture is in the solid phase. Specific heat studies by Tognon (1968) indicate that a small amount of evaporable moisture may exist in the liquid state down to 178 K.

The upper and lower specimens experienced different temperature gradients during cool-down due to the configuration of the system. The temperature profile for the initial cool-down is shown in figure 3. As seen in this figure, the temperature gradients, as well as the cooling rate, differed for the two specimens. Migration of moisture within each specimen is a function of the temperature difference until the freezing point of the internal moisture is reached. Redistribution of moisture within the specimens is expected to be small during the time required to reach very low temperatures.

4. EXPERIMENTAL RESULTS

The thermal conductivity results represent the mortar with three different moisture contents. The initial average moisture content, as estimated above, was 10.4 percent of the dry specimen weight. Figure 4 (\diamond and $*$) shows the data for the mortar in this condition. The average specimen temperature was above 269 K for approximately 6.5 h while taking the data shown in this figure. The relatively low temperatures encountered and the reduced, exposed specimen area which exists when the specimens are in the stacked configuration shown in figure 2, limited moisture loss during this time. Some redistribution of the moisture could be expected with the migration toward the low-temperature surface. The temperature of the data points shown in figure 4 does not, in general, reflect the order in which they were taken. The excursion to temperatures higher than 273 K made no detectable change in the thermal conductivity at lower temperatures.

Experimentally, the temperature range between 225 and 235 K was very difficult for the specimens with 10.4 percent evaporable moisture. Equilibrium conditions were tenuous compared to those outside this range. The results in this range, shown as ($*$), are significantly less precise than the data taken at higher and lower temperatures. The sequence of observations in this range, in order of decreasing conductivity, was run 13, run 22, run 14, and run 9; these data were taken over a period of 3.2 days.

The second set of data (\bullet) shown in this figure was determined after the specimens had been conditioned at temperatures higher than 273 K for approximately 20 h. This treatment was intended to alter the moisture content and distribution enough to make an observable, but not extreme, change in λ . The conductivity decreased by 2.5 percent when the gradient conditions at 317 K were held for 15 hours ($+$).

Subsequent to these tests, the temperature of the specimens was maintained at $325 \leq T \leq 330$ K for 72 hours while the system pressure was reduced to less than 26 kPa. The system was purged with dry nitrogen gas several times during this period. This procedure was intended to produce a severe loss of moisture from the specimens. The thermal conductivity data shown in figure 4 (\blacktriangle) were taken with the specimens in this condition.

Immediately following the third series of measurements, the specimens were removed from the system and weighed. The moisture content was found to be 4 percent of the dry specimen weight.

5. DISCUSSION

The current data are compared to values found in the literature in figures 5 and 6 for moist and dry cementitious materials respectively. Although the composition of the specimens used for these curves differs significantly, the conductivity of the dry specimens (fig. 6) follow the general rule that conductivity increases with increasing density (Tye and Spinney, 1976). This rule is not strictly applicable to moist materials as is seen in figure 5.

A survey of the literature on λ of concrete at low temperatures indicates that the peak in λ of the saturated specimens at 232 K (fig. 4- \diamond , $*$) has not been previously observed. This may be due to the coarse grid of points in past experiments. The 10% increase in λ appears much like that seen in the specific heat of a material undergoing a lambda transition. Since λ is related to specific heat by

$$\lambda = \rho \alpha C_p \quad (2)$$

where α is diffusivity and ρ is density, several differential scanning calorimeter (DSC)

determinations of C_p were made on materials similar to the λ specimens. Our limited investigation did not reveal a singular transition capable of causing the peak at 232 K. Further tests utilizing DSC and thermal gravimetric analysis (TGA) will be made on the NBS-mortar specimens in order to characterize the complex, interdependent reactions which occur as the temperature is lowered and which affect the thermal properties. Similar techniques were used by Stockhausen, et al. (1979) and by Tognon (1968). Stockhausen observed a strong transition at 230 K in a hardened cement paste, and Tognon quantitatively described the freezing process in a moist cement paste. Any model describing thermal transport in concrete must account for the relative amount of solid and liquid phases present as a function of temperature.

The evaporable moisture, water containing various dissolved salts, is distributed throughout the hydrated material in pores and capillaries of widely varying sizes. The freezing process occurs over a wide range of temperatures. Freezing first takes place in the larger pores and is accompanied by short range migration of moisture from small pores. This process begins at about 269 K and continues until roughly 200 K at which temperature most evaporable moisture is in the solid phase (Tognon, 1968).

Anomalies or inflections in other low-temperature properties at about 230 K and 269 K have been observed. Tognon (1968), Goto and Miura (1979), and Rostasy, Schneider, and Wiedemann (1979) found sharp changes in $\Delta L/L$ of moist concrete in this temperature range. Tognon also found rapid changes in the flexural and compressive strengths in this temperature range. Although the consensus is that the observed behavior is due to the presence and effect of evaporable moisture in the cementitious materials, no detailed model has yet been developed.

Changes observed in $\Delta L/L$ of a given specimen as it is thermally cycled to low temperature are attributed to progressive alteration of the pore structure. These changes cause hysteresis during a single cooling-warming cycle and magnitude shifts for repeated cycles. The internal pore damage was studied by Rostasy, Weiss, and Wiedemann (1980), who found that the total pore volume was not greatly affected by thermal cycling to cryogenic temperatures, but that the distribution of pore radii increased significantly in the 500 - 15000 Å sizes. This redistribution to larger pores would be expected to change the ice-liquid composition at a given temperature and change the concomitant thermal conductivity. This effect cannot be unambiguously separated from the mild moisture loss occurring between the first two sets of λ data (fig. 4-◇,●). The inflection points for the second (less moist) set of data are shifted to lower temperatures and are substantially broadened. This may be the result of moisture loss and/or alteration of the pore radius. The 2.9 percent decrease in conductivity at 165 K, where all moisture is in the solid state, indicates that a net moisture decrease did occur between the first and second set of data. Further testing involving multiple thermal cycles in the temperature range where only negligible moisture loss occurs is necessary to quantitatively determine the effect of thermal cycling on λ .

The third set of data, taken after aging at high temperatures and reduced pressure, indicates a much lower conductivity (fig. 4-▲). This is the expected, qualitative effect of a large reduction in moisture content. This large change in moisture content results in both a reduction in magnitude of λ and a different characteristic λ versus T shape (fig. 4). In comparing the data from the "moderately wet" (●) and "dry" (▲) specimens one finds the double inflection curve between 180 and 300 K replaced by a curve with a single inflection. The conductivity in the range above 310 K is reduced in magnitude for the dry specimen relative to the moist specimen conductivity by about 33 percent, but retains the slight positive slope. At 165 K the reduction is 28 percent.

6. CONCLUSION

The thermal conductivity of porous, moist materials can be measured utilizing guarded-hot-plate systems provided the test temperatures are low enough to cause partial freezing of the moisture in the pores. The magnitude of λ for the NBS-mortar specimens is moisture dependent and is reasonable for a material of this type and density.

Two details were found which are not seen in the very limited literature data for low temperature λ : (1) The moist specimens clearly show inflections at temperatures near 270 K and 232 K. The slope change at 270 K is thought to be due to the initial freezing of

moisture in the larger pores. The increasing conductivity as temperature decreases in the range 270 K to 232 K probably reflects the continuous freezing process in pores of decreasing radius. Other properties, particularly thermal strain, also exhibit inflections and/or discontinuities at these temperatures. (2) The conductivity for both moist and dry mortar decreases at a faster rate than previously observed when the temperature is below 232 K. There is insufficient data available at the present time to develop a model for this behavior.

7. REFERENCES

- ASTM (1978). Annual Book of ASTM Standards. American Society for Testing Materials, Philadelphia, PA.
Standard C114-77, Chemical analysis of hydraulic cement, Part 13.
Standard C138-77, Unit weight, yield, and air content (gravimetric) of concrete, Part 14.
Standard C150-78, Specification for portland cement, Part 14.
Standard C177-76, Steady-state thermal transmission properties by means of the guarded hot plate, Part 18.
Standard C192-76, Making and curing concrete test specimens in the laboratory, Part 14.
Standard C204-78, Fineness of portland cement by air permeability apparatus, Part 13.
Standard C266-77, Time of setting of hydraulic cement by Gillmore needles, Part 13.
- Goto, Y., and Miura, T. (1979). Deterioration of concrete subjected to repetitions of very low temperatures. In Proceedings of the Japanese Concrete Institute, Japan Concrete Institute, Tokyo.
- Lentz, A. E., and Monfore, G. E. (1965). Thermal conductivity of concrete at very low temperatures. *Journal of PCA Res. and Dev. Labs.* 7, 39-46.
- Lentz, A. E., and Monfore, G. E. (1966). Thermal conductivities of portland cement paste, aggregate and concrete down to very low temperatures. *Journal of PCS Res. and Dev. Labs.* 8, 27-33.
- Monk, E. F. (1975). Petrographic examination of Clear Creek Aggregate. U.S. Bureau of Reclamation, Denver, CO.
- Richard, T. G. (1977). Low temperature behavior of cellular concrete. *ACI Journal*, 173-178.
- Rostasy, F. S., Schneider, U., and Wiedemann, G. (1979). Behavior of mortar and concrete at extremely low temperatures. *Cem. Concr. Res.* 9, 365-376.
- Rostasy, F. S., Weiss, R., and Wiedemann, G. (1980). Changes of pore structure of cement mortars due to temperature. *Cem. Concr. Res.* 10, 157-164.
- Smith, D. R., Hust, J. G., and Van Poolen, L. J. (1981). A guarded-hot-plate apparatus for measuring effective thermal conductivity of insulations between 80 K and 360 K. Nat. Bur. of Stand. (U.S.) NBSIR to be published.
- Somers, E. V., and Cyphers, J. A. (1951). Analysis of errors in measuring thermal conductivity of insulating materials. *Rev. Sci. Instrum.* 22, 583-586.
- Stockhausen, N., Dorner, H., Zech, B., Setzer, M. J. (1979). Untersuchung von gefriervorgängen in zementstein mit hilfe der DTA. (Freezing phenomena in hardened cement paste were investigated by DTA). *Cem. Concr. Res.* 9, 783-794.
- Tognon, G. (1968). Supplementary paper III - 24: Behavior of mortars and concretes in the temperature range from +20°C to -196°C. The Cement Association of Japan, Tokyo.
- Trujillo, R. (1980). Martin Marietta Cement Co., Lyons, Colorado. Private Communication.
- Tye, R. P., and Spinney, S. C. (1976). Thermal conductivity of concrete: measurement problems and effect of moisture. *Bull. Inst. Int. Froid, Annexe 1976-2*, 119-127.
- Zemansky, M. W. (1968). Heat and Thermodynamics, McGraw-Hill, New York.

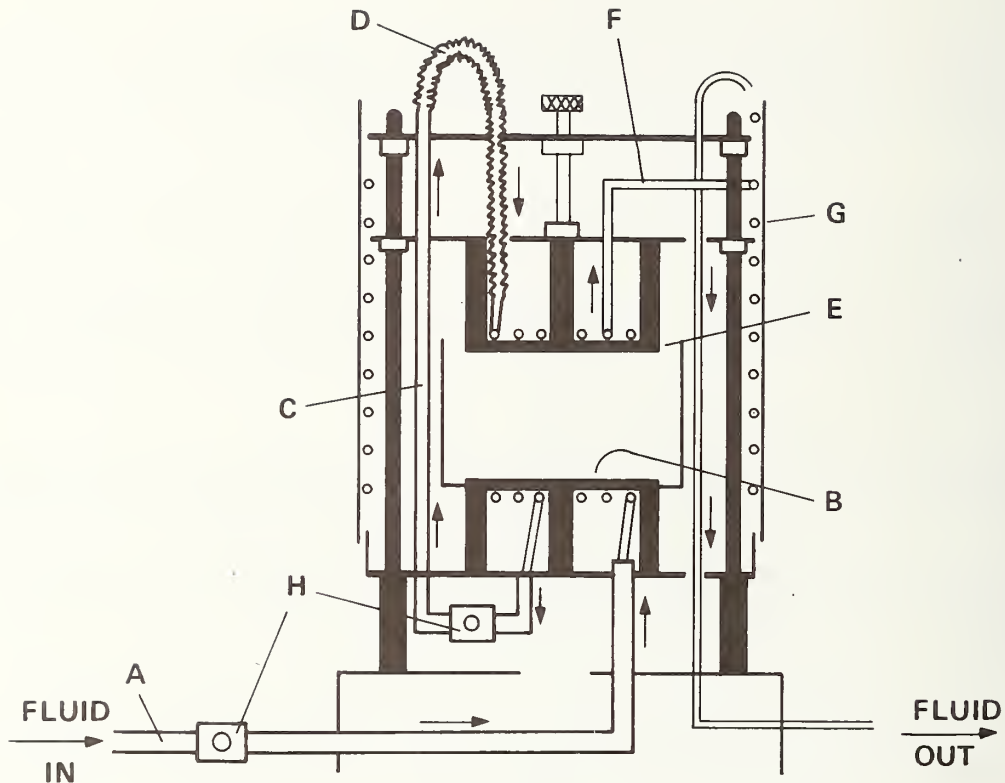


Figure 1. Schematic of guarded-hot-plate thermal conductivity apparatus. A, vacuum insulated transfer tube; B, bottom cold plate; C, vacuum insulated transfer tube; D, flex tubing; E, top cold plate; F, transfer tube; G, shroud cooling tubes; H, throttle valves.

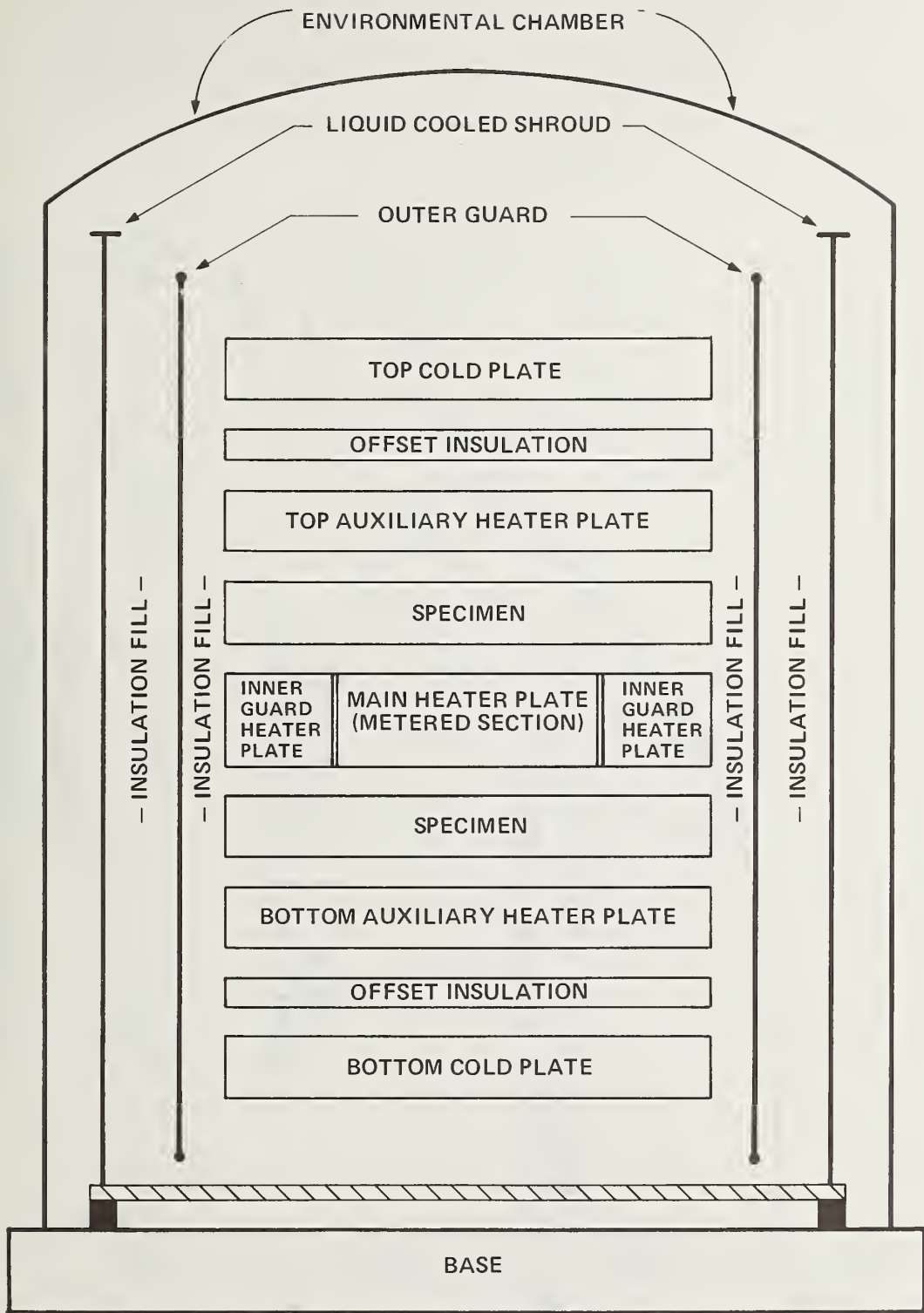


Figure 2. Schematic of guarded-hot-plate specimen configuration and environmental chamber.

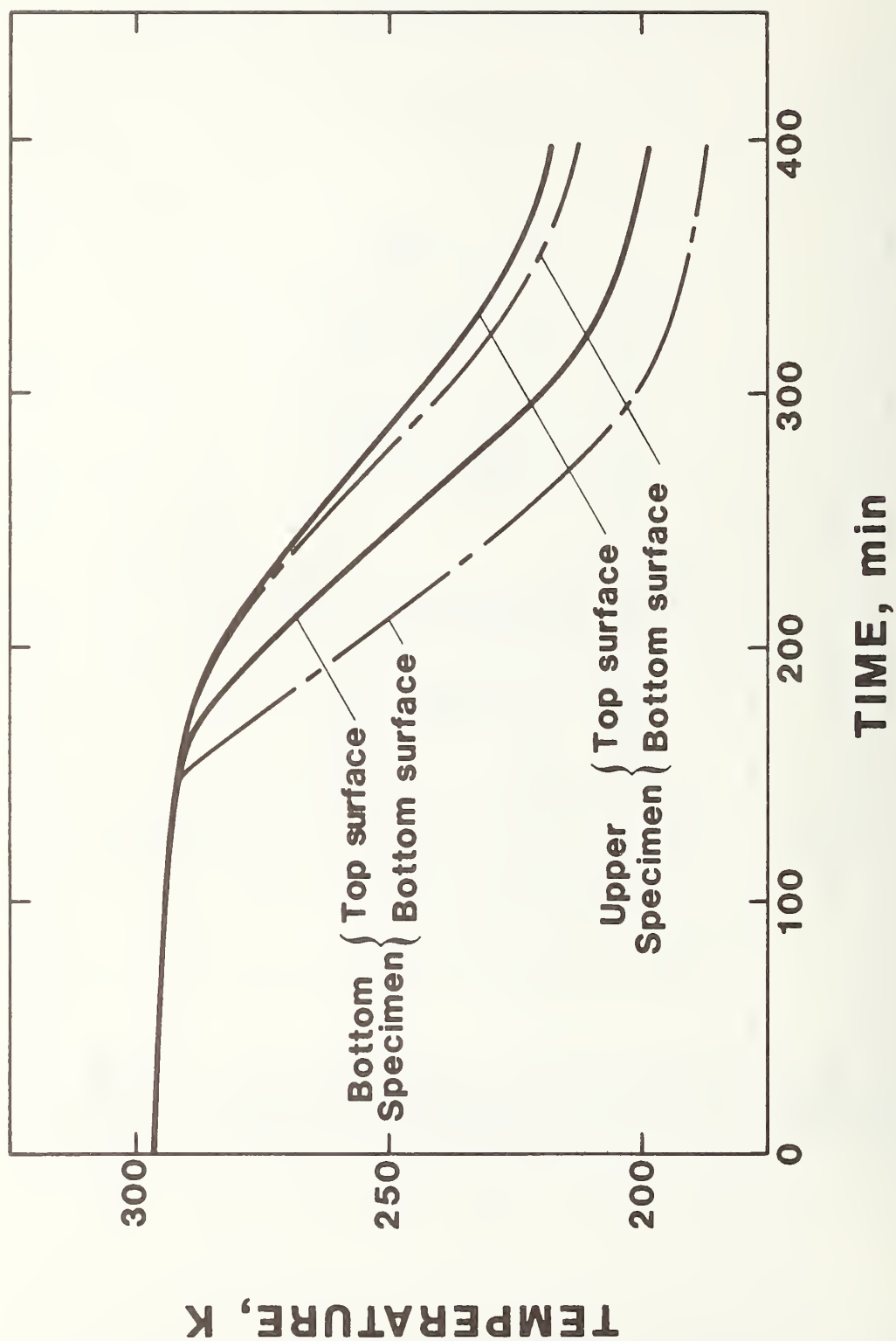


Figure 3. Initial cooling profiles for concrete mortar specimens after being installed in guarded-hot-plate apparatus.

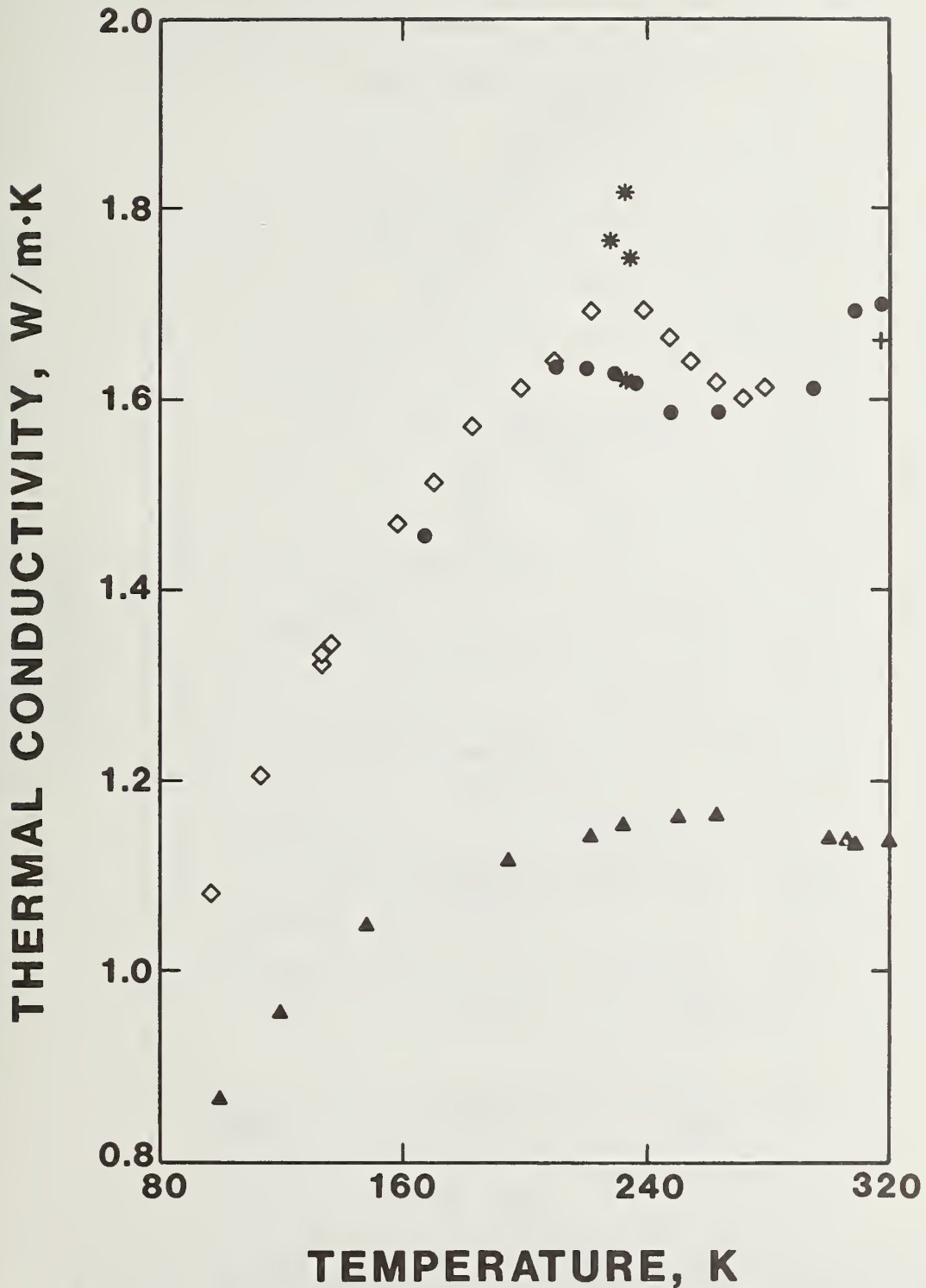


Figure 4. Thermal conductivity as a function of temperature for a concrete mortar with three different moisture contents: ◇, 10.4 percent moisture; ●, slightly less than 10.4 percent moisture; ▲, 4 percent moisture. Data points of reduced precision are indicated by (*). The conductivity of the slightly dried specimen decreased by 2.5 percent (+) when the gradient conditions at 317 K were held for 15 hours.

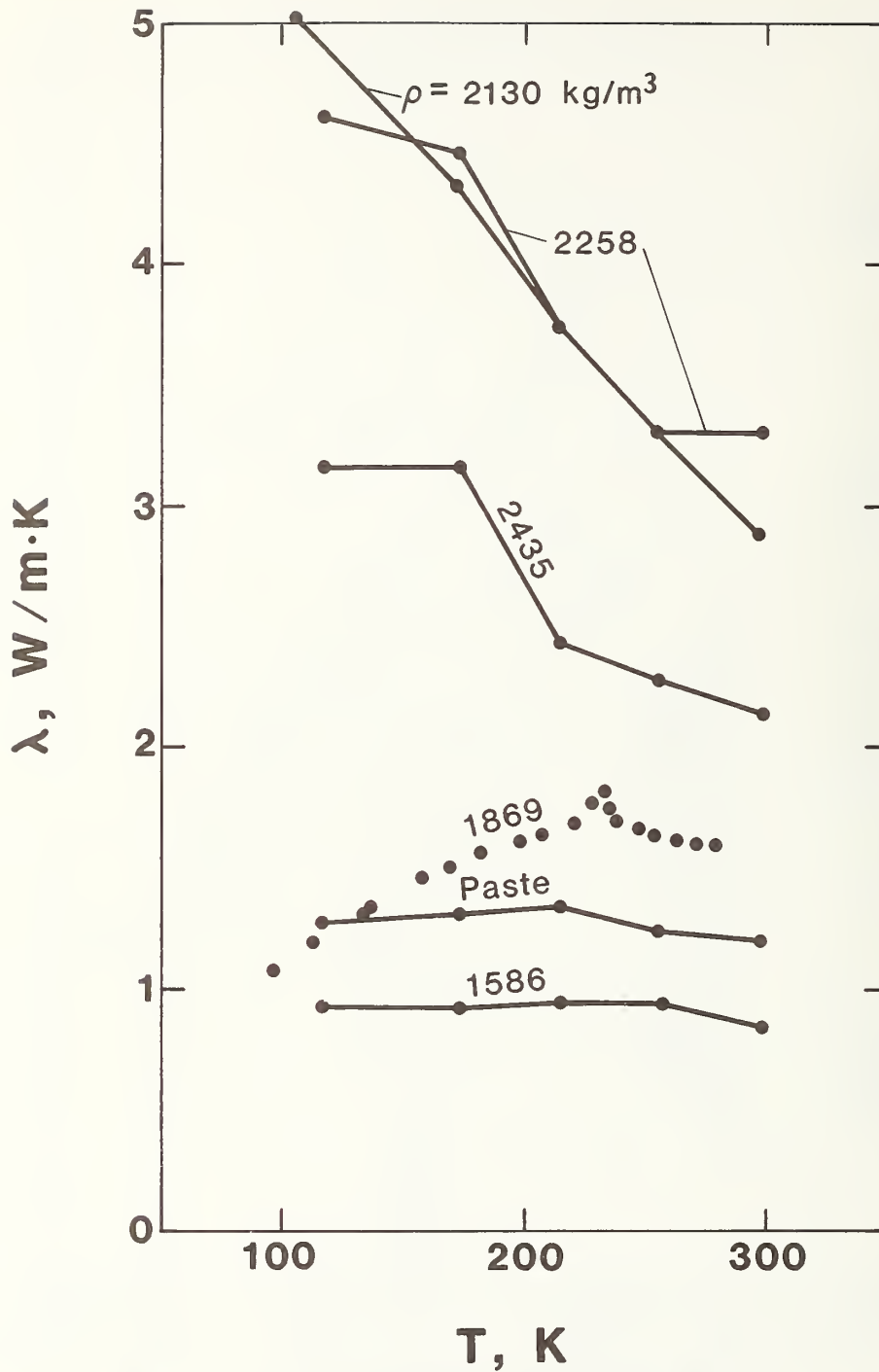


Figure 5. Thermal conductivity as a function of temperature for various cementitious materials in moist conditions: $\rho=2130 \text{ kg/m}^3$, sandstone concrete; $\rho=2258 \text{ kg/m}^3$, Elgin sand and gravel concrete; $\rho=2435 \text{ kg/m}^3$, marble concrete; portland cement paste; $\rho=1586 \text{ kg/m}^3$, expanded shale concrete (Lentz and Monfore, 1965, 1966);, NBS mortar.

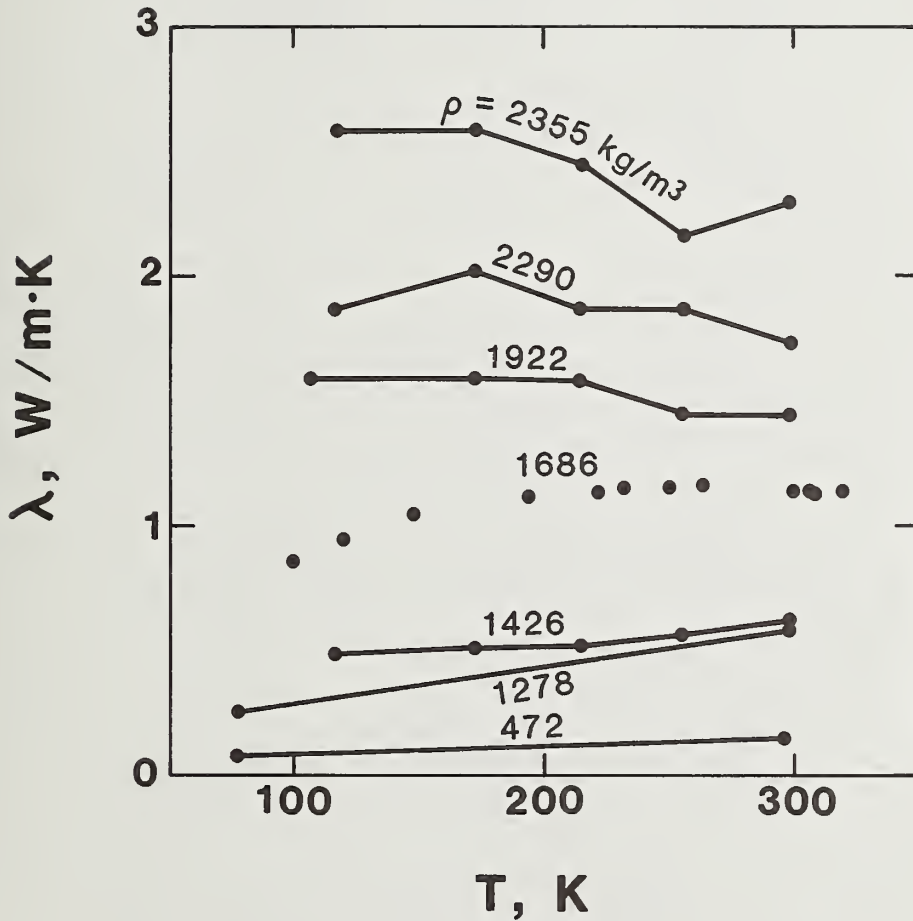


Figure 6. Thermal conductivity as a function of temperature for various cementitious materials in relatively dry conditions: $\rho=2355 \text{ kg/m}^3$, Elgin sand and gravel concrete; $\rho=2290 \text{ kg/m}^3$, marble concrete; $\rho=1922 \text{ kg/m}^3$, sandstone concrete; $\rho=1426 \text{ kg/m}^3$, expanded shale concrete (Lentz and Monfore, 1965, 1966); $\rho=1278, 472 \text{ kg/m}^3$, cellular concrete (Richard, 1977); ..., NBS mortar.

U.S. DEPT. OF COMM. BIBLIOGRAPHIC DATA SHEET <i>(See instructions)</i>	1. PUBLICATION OR REPORT NO. NBSIR 81-1651	2. Performing Organ. Report No.	3. Publication Date October 1981
4. TITLE AND SUBTITLE THERMAL CONDUCTIVITY OF A CONCRETE MORTAR FROM 95 K to 320 K			
5. AUTHOR(S) L. L. Sparks			
6. PERFORMING ORGANIZATION <i>(If joint or other than NBS, see instructions)</i> NATIONAL BUREAU OF STANDARDS DEPARTMENT OF COMMERCE WASHINGTON, D.C. 20234		7. Contract/Grant No.	8. Type of Report & Period Covered
9. SPONSORING ORGANIZATION NAME AND COMPLETE ADDRESS <i>(Street, City, State, ZIP)</i> Maritime Administration Department of Commerce Building Washington, DC 20235			
10. SUPPLEMENTARY NOTES <input type="checkbox"/> Document describes a computer program; SF-185, FIPS Software Summary, is attached.			
11. ABSTRACT <i>(A 200-word or less factual summary of most significant information. If document includes a significant bibliography or literature survey, mention it here)</i> <p>The thermal conductivity of a single concrete mortar specimen with varying moisture content is reported in the temperature range from 95 to 320 K. The measurements were made in a guarded-hot-plate apparatus (ASTM C-177). Moisture migration caused by temperature gradients was minimized by studying the saturated specimen in the low-temperature region. Specimen moisture content and concomitant thermal conductivity were altered by imposing low-pressure, high-temperature conditions on the specimen. The effect of changing the moisture content is discussed.</p>			
12. KEY WORDS <i>(Six to twelve entries; alphabetical order; capitalize only proper names; and separate key words by semicolons)</i> concrete; guarded hot plate; low temperature; moisture migration; mortar; porous solid; thermal conductivity.			
13. AVAILABILITY <input checked="" type="checkbox"/> Unlimited <input type="checkbox"/> For Official Distribution. Do Not Release to NTIS <input type="checkbox"/> Order From Superintendent of Documents, U.S. Government Printing Office, Washington, D.C. 20402. <input checked="" type="checkbox"/> Order From National Technical Information Service (NTIS), Springfield, VA. 22161			14. NO. OF PRINTED PAGES 16 15. Price \$5.00

